

IMPROVING HYPERSPECTRAL ADVERSARIAL ROBUSTNESS USING ENSEMBLE NETWORKS IN THE PRESENCES OF MULTIPLE ATTACKS

Nicholas Soucy and Salimeh Yasaei Sekeh

Department of Computer Science, SCIS, University of Maine, Orono, USA

ABSTRACT

Semantic segmentation of hyperspectral images (HSI) has seen great strides in recent years by incorporating knowledge from deep learning RGB classification models. Similar to their classification counterparts, semantic segmentation models are vulnerable to adversarial examples and need adversarial training to counteract them. Traditional approaches to adversarial robustness focus on training or retraining a single network on attacked data, however, in the presence of multiple attacks these approaches decrease the performance compared to networks trained individually on each attack. To combat this issue we propose an *Adversarial Discriminator Ensemble Network* (ADE-Net) which focuses on attack type detection and adversarial robustness under a unified model to preserve per data-type weight optimally while robustifying the overall network. In the proposed method, a discriminator network is used to separate data by attack type into their specific attack-expert ensemble network. Our approach allows for the presence of multiple attacks mixed together while also labeling attack types during testing. We experimentally show that ADE-Net outperforms the baseline, which is a single network adversarially trained under a mix of multiple attacks, for HSI Indian Pines, Kennedy Space, and Houston datasets.

Index Terms— Adversarial Examples, Adversarial Robustness, Deep Neural Network, Hyperspectral Images, Semantic Segmentation

1. INTRODUCTION

In recent years hyperspectral imaging has seen rapid growth with the push to semantically label each pixel. However, these state-of-the-art semantic segmentation neural networks are quite vulnerable to the addition of imperceptible perturbations to the input data [1]. These perturbations are often well-crafted attacks that when added in small amounts to an input image, drastically fool the network and decrease the accuracy of the prediction [2]. To combat this challenge and make the network robust toward attacks, adversarial training is performed on the network. The main philosophy behind adversarial training is to make the current trained network, or a new network, classify attacked and non-attacked samples accurately. To achieve this, one generates the adversarial

examples and then either continually trains the trained network, or mixes the attack examples with non-attacked examples and trains a new network from scratch [3, 4]. However, in this approach, the network performs worse on each individual data attack type due to the updated weights, but better overall. Another approach is to detect the attacked data to avoid it during classification. Adversarial detection focuses on using a trained network or feature space analysis to determine if a sample is under attack or not. In this case, the attacks are often ignored, despite having information that might be valuable to classify [5]. In this work, we fuse the strengths of these two approaches while removing their weaknesses. In our approach, we use attack-type detection and utilize it in semantic segmentation. After each sample is separated based on the attack type, our ensemble model classifies attacks individually so that each sub-network is an expert at a particular attack, thereby preserving the optimal decision boundaries for the classification task.

Contribution: (1) Explore the effects of adversarial examples on semantic segmentation with multiple attacks present and use the ensemble method to make a class label prediction. (2) Utilize the similarity measure Centered Kernel Alignment (CKA) on logits to assist in attack labeling in the discriminator phase. (3) Develop a novel ADE-Net model that can use any semantic segmentation network while classifying attack type and class type in one unified model.

2. RELATED WORKS

Adversarial Robustness: In [6] the authors showed that adding a small well-crafted perturbation to a sample can be catastrophic to a network’s performance. These adversarially attacked images often look the same to a human observer but make the network vulnerable. The study of adversarial examples and robustness in HSI semantic segmentation is a new entry into the field with [7] being the first to introduce the idea of adversarial attack-defense in the HSI domain. They applied the Fast Gradient Signed Method (FGSM) [8], Carlini and Wagner (CW) [9], and Projected Gradient Decent (PGD) [10] to HSIs. In addition, they created a self-attention context network (SACNet) to better defend against these attacks. The authors in [11] use their Masked Spatial-Spectral Autoencoder (MSSA) which consists of masked sequence attention learning, dynamic graph embedding, and self-supervised re-

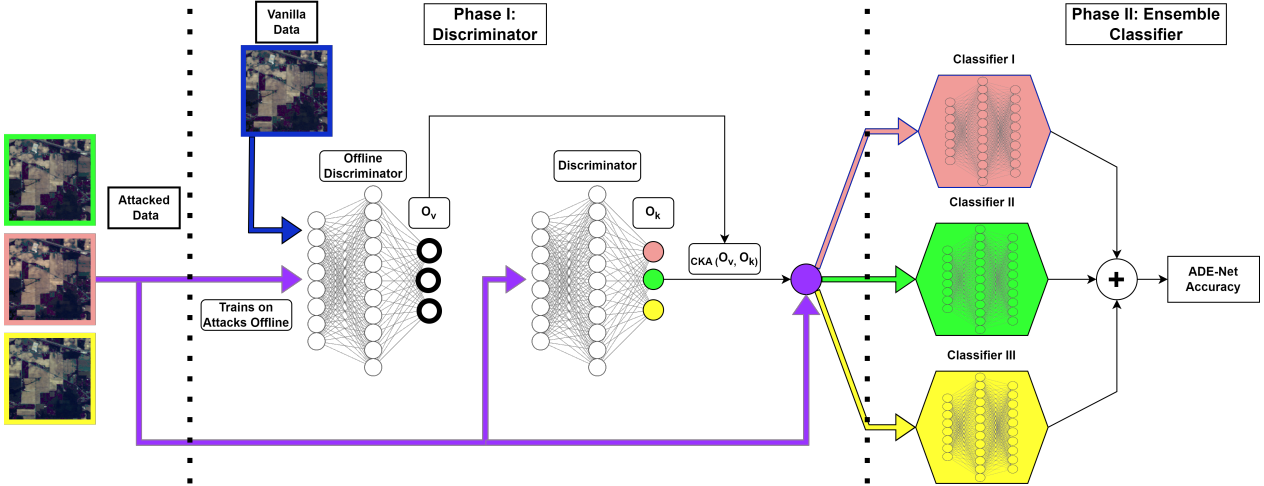


Fig. 1. Overview of ADE-Net model structure: **Phase I** contains the Discriminator Network and **Phase II** contains the Ensemble Networks. The colors represent different attacks FGSM (green), C&W (pink), PGD (yellow), and blue is vanilla data. The purple line represents a mix of the attack data. Phase I labels samples by attack type, and Phase II labels samples by class type. O_v is generated using an offline trained discriminator. Then during training, the CKA (1) is calculated from the logits of each classified attack, O_k , with the offline O_v to use information from deeper layers in the network to aid in attack labeling.

construction. Rather than focusing on semantic segmentation via network architecture, some works like [12, 13] try to use the rich spectral information to robustify the entire process. In [12], they propose a spectral sampling and shape encoding to increase adversarial robustness as a preprocessing step to traditional per-pixel classification via random sampling. In work [13], rather than random sampling, they use autoencoders to reconstruct the spectral signature of pixels for later classification with a shared global loss function. However, all these approaches focus on a single attack at a time and do not explore network robustness in the presence of multiple attacks. Recently, AutoAttack [14] extends PGD to create an aggregate attack and achieves lower robust networks. A union of attacks similar to AutoAttack is created in [15] by using a generalized PGD-based procedure to incorporate multiple perturbation models into a single attack which also leads to drastically worse performance than individual perturbations. Many existing works use these aggregate attacks now to test performance, but still, test one aggregate attack at a time.

Ensemble Methods: In HSI semantic segmentation, the more successful ensemble models have focused on using individual networks that work in parallel on sub-sets of the data for better overall performance [16, 17, 18, 19]. The ensemble EECNN method [16] applies a random sampling technique on the feature space to obtain the data subsets for each submodel. Further, TCNN-E-ILS [17] uses an ensemble technique and does not use an intelligent method of discriminating data for each network. Both EECNN and TCNN-E-ILS do not train under a shared loss function whereas, in our ADE-Net, the discriminator intelligently splits attack types for each ensemble and through a shared loss function, the individual ensemble network can share information.

3. PROPOSED METHOD: ADE-NET

In this section, we give an overview of our main problem setup and model solution. Later we use that notation to develop our proposed ADE-Net.

Notation: Consider vanilla data as $\{x_i^v, y_i^v\}_{i=1}^{n_v}$ with size n_v . Define attack label $k = 1, \dots, K$ and consider k -th attack data $\{x_i^k, y_i^k\}_{i=1}^{n_k}$ with size n_k . Each attacked point has two labels: class label and attack label, $\{x_i^k, y_i^k, c_i = k\}_{i=1}^{n_k}$. For a classifier F , consider a discriminator F_D that focuses on separating input based on attack type, and ensemble classifiers F_k , which denotes the k -th classifier expert in attack type k . For each ensemble network, ω_k^* is the optimal weight of F_k , and ω_D^* is the optimal weight of F_D on all K attack data. Let $O_v \in \mathcal{R}^{m \times n_v}$ be the logits of passing vanilla on an offline trained F_D on attacks, and $O_k \in \mathcal{R}^{m \times n_k}$ be the logits of F_D on single attack k .

Centered Kernel Alignment: In ADE-Net, we use a network-layer similarity measure called Centered Kernel Alignment (CKA) [20] as follows:

$$CKA(O_v, O_k) = \frac{\|(O_v)^T O_k\|_F^2}{\|(O_v)^T O_v\|_F^2 \|(O_k)^T O_k\|_F^2}, \quad (1)$$

For this particular use of CKA, we are using vanilla logits O_v from a discriminator trained offline on attacks to determine the dissimilarity between different attacks. O_k is calculated during training where k is the assigned attack type for each sample during training by the discriminator. CKA was chosen for its intuition over other similarity measures to aid our attack separation. Adversarial attacks have a prevalent effect on a network in deeper layers, therefore, once CKA calculates the relative dissimilarity between the logits of vanilla data and

attacked data, we have an intuitive measure to use attack information in the logit space rather than just the feature space.

Methodology: For ADE-Net, our overall model structure consists of two phases: Phase I Discriminator and Phase II Ensemble. Fig. 1 presents a visual overview of ADE-Net.

Discriminator Phase I: The aim of the discriminator is to add adversarial detection to ADE-Net via attack type classification and CKA to separate mixed attack data. For discriminator, we use a categorical cross-entropy loss function as $\omega_D^* = \arg \min_{\omega_D} \mathcal{L}_{\omega_D}(F_D(\mathbf{x}))$. To increase attack classification accuracy further, we use the similarity measure CKA from 1 to incorporate more information about attacks into the loss function. This term is the sum of CKAs between logit-layer vanilla data output on a trained discriminator, and the logit-layer output of each attack present during training. The optimal ω_D^* is learned by solving the optimization problem:

$$\arg \min_{\omega_D} \beta \mathcal{L}_{\omega_D}(F_D(\mathbf{x})) + \sum_{k=1}^K \lambda_k CKA(O_v, O_k),$$

where λ_k and β are hyperparameters and \mathcal{L}_{ω_D} is the cross-entropy function on attack labels while also incorporating the similarity of the attack compared to non-attack data in deeper layers of a trained network.

Ensemble Phase II: The ensemble phase is constituted by a number of networks, equal to n_k , that focus on regular class label classification. Each network is an expert at a particular attack determined by the output label from the discriminator. We use an ensemble categorical cross-entropy loss

function $\omega_k^* = \arg \min_{\omega_k} \sum_{k=1}^K \alpha_k \mathcal{L}_{\omega_k}(F_k(\mathbf{x}), y)$, where α_k , $k = 1, \dots, K$ are hyperparameters and allow for individual networks to get more attention than others.

Unified ADE-Net: We propose in ADE-Net that the ensemble classifiers are trained collaboratively with the discriminator focusing on class and attack classification respectively:

$$\omega_D^*, \omega_k^* = \arg \min_{\omega_D, \omega_k} \sum_{k=1}^K \alpha_k \mathcal{L}_{\omega_k}(F_k(\mathbf{x}), y) \quad (2)$$

$$+ \sum_{k=1}^K \lambda_k CKA(O_v, O_k) + \beta \mathcal{L}_{\omega_D}(F_D(\mathbf{x}), c), \quad (3)$$

where terms in (3) is for discriminator phase and the term in (2) is for the ensemble phase. The overview of our ADE-Net algorithm is shown in Algorithm 1:

4. EXPERIMENTS

Datasets: For our experiments, we use three HSI datasets: Indian Pines (IP), Kennedy Space Center (KSC) [21], and Houston [22]. Patching is not used. Each dataset is reduced to 30 bands using Principal Component Analysis (PCA).

Training: We use U-Net [23] for the discriminator and all ensemble networks. We use Adam optimizer with a learning

Algorithm 1: ADE-Net model

Input: Data $\{x_i, y_i\}_{i=1}^N$. Set K, E : # of attacks and epochs. Learning rates η_D and η_j , $j = 1, \dots, K$.

Output: Overall Test Accuracy

Attack data $\{x_i, y_i\}_{i=1}^N$ with k attack types to get $\{x_i^k, y_i^k, c_i = k\}_{i=1}^{n_k}$ and vanilla data $\{x_i^v, y_i^v\}_{i=1}^N$. Train Discriminator F_D on attacked training data offline and pass vanilla and logits O_v . Shuffle attack data $\{x_i^k, y_i^k, c_i = k\}_{i=1}^{n_k}$ (including vanilla data).

for $e = 1, \dots, E$ **do**

for $b = \text{batch}_1, \dots, \text{batch}_B$ **do**

Input data into F_D on the attack type and compute $CKA(O_v, O_k)$. Update F_D 's weights as $\omega_D \leftarrow \omega_D - \eta_D \nabla_{\omega_D} (3)$

Discriminate attacks based on the ω_D .

for $j = 1, \dots, k$ **do**

Input $\{x_i^j, y_i^j, c_i = j\}_{i=1}^{n_j}$ discriminated by F_D into F_j . Update classifier F_j weights as $\omega_j \leftarrow \omega_j - \eta_j \nabla_{\omega_j} (2)$

end

end

Report Acc

rate of 0.001 for all networks under three trials. We use a batch size of 256 we train ADE-Net for 100 epochs. The offline discriminator training is 25 epochs.

Attacks: For attacks, we use the Fast Gradient Signed Method (FGSM) [8], Carlini and Wagner (CW) [9], Projected Gradient Decent (PGD) [10], and Iterative Fast Gradient Signed Method (I-FGSM) [24]. In our experiments '2 attack' is FGSM + CW, '3 attack' is '2 attack' + PGD, '4 attack' is '3 attack' + I-FGSM, and finally '5 attack' is '4 attack' + vanilla data. All attacks were generated using $\epsilon = 0.1$.

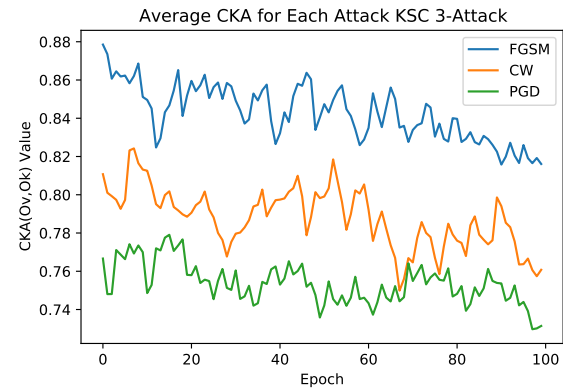


Fig. 2. Comparison of attacks' CKA values calculated from the average of each batch for each FGSM, CW, and PGD attack during ADE-Net training for the KSC dataset. Note that for each epoch the three attacks are consistently separated.

# Attack	All = 1.0	$\lambda_k=\beta=0.1$ $\alpha_k=10.0$	$\lambda_k=\beta=10.0$ $\alpha_k=0.1$	$\lambda_k=\beta=1.0$ $\alpha_k=X_k$	$\lambda_k=0$ (No CKA) $\beta=\alpha_k=1.0$	Baseline
2	I: 95.29 \pm 0.01 II: 80.37 \pm 0.01	I: 95.19 \pm 0.04 II: 80.00 \pm 0.01	I: 95.34 \pm 0.03 II: 80.11 \pm 0.02	I: 95.21 \pm 0.04 II: 80.30 \pm 0.01	I: 95.00 \pm 0.05 II: 79.67 \pm 0.02	78.78 \pm 0.08
	I: 63.97 \pm 0.03 II: 81.57 \pm 0.02	I: 64.12 \pm 0.04 II: 81.71 \pm 0.02	I: 63.97 \pm 0.04 II: 81.62 \pm 0.03	I: 63.99 \pm 0.03 II: 81.72 \pm 0.02	I: 63.50 \pm 0.04 II: 81.49 \pm 0.04	80.11 \pm 0.13
3	I: 48.03 \pm 0.04 II: 82.23 \pm 0.12	I: 47.98 \pm 0.10 II: 82.06 \pm 0.11	I: 47.98 \pm 0.09 II: 82.1 \pm 0.12	I: 48.05 \pm 0.05 II: 82.51 \pm 0.09	I: 47.51 \pm 0.10 II: 81.66 \pm 0.14	81.37 \pm 0.02
	I: 50.30 \pm 0.03 II: 83.27 \pm 0.15	I: 50.40 \pm 0.02 II: 83.27 \pm 0.14	I: 50.45 \pm 0.03 II: 83.17 \pm 0.16	I: 50.30 \pm 0.03 II: 83.55 \pm 0.13	I: 50.40 \pm 0.04 II: 83.10 \pm 0.16	82.65 \pm 0.22
2	I: 100.0 \pm 0.0 II: 87.45 \pm 0.39	I: 100.0 \pm 0.0 II: 86.87 \pm 0.38	I: 100.0 \pm 0.0 II: 86.94 \pm 0.29	I: 99.98 \pm 0.01 II: 87.63 \pm 0.24	I: 99.54 \pm 0.02 II: 86.01 \pm 0.36	83.59 \pm 0.40
	I: 98.3 \pm 0.04 II: 88.07 \pm 0.04	I: 97.90 \pm 0.06 II: 87.39 \pm 0.09	I: 97.73 \pm 0.03 II: 88.00 \pm 0.05	I: 97.70 \pm 0.04 II: 87.20 \pm 0.08	I: 97.45 \pm 0.05 II: 87.11 \pm 0.10	84.69 \pm 0.32
3	I: 73.30 \pm 0.10 II: 88.18 \pm 0.12	I: 74.04 \pm 0.08 II: 88.65 \pm 0.08	I: 74.21 \pm 0.10 II: 88.22 \pm 0.09	I: 73.39 \pm 0.12 II: 88.50 \pm 0.10	I: 73.44 \pm 0.10 II: 88.00 \pm 0.12	86.12 \pm 0.14
	I: 78.57 \pm 0.01 II: 88.73 \pm 0.11	I: 78.66 \pm 0.03 II: 88.25 \pm 0.12	I: 79.07 \pm 0.02 II: 88.66 \pm 0.13	I: 78.68 \pm 0.04 II: 88.75 \pm 0.09	I: 78.01 \pm 0.04 II: 87.89 \pm 0.13	86.46 \pm 0.17
2	I: 98.61 \pm 0.29 II: 95.84 \pm 0.59	I: 98.87 \pm 0.22 II: 96.24 \pm 0.54	I: 98.18 \pm 0.19 II: 95.28 \pm 0.61	I: 98.16 \pm 0.21 II: 95.38 \pm 0.49	I: 98.11 \pm 0.22 II: 95.22 \pm 0.53	93.94 \pm 0.12
	I: 67.05 \pm 0.05 II: 96.32 \pm 0.49	I: 66.81 \pm 0.06 II: 95.77 \pm 0.35	I: 67.24 \pm 0.05 II: 95.70 \pm 0.44	I: 67.20 \pm 0.05 II: 95.94 \pm 0.48	I: 67.03 \pm 0.07 II: 95.89 \pm 0.42	95.15 \pm 0.05
3	I: 50.51 \pm 0.06 II: 96.02 \pm 0.16	I: 50.47 \pm 0.06 II: 97.21 \pm 0.09	I: 50.40 \pm 0.05 II: 96.10 \pm 0.11	I: 50.52 \pm 0.04 II: 97.24 \pm 0.08	I: 50.39 \pm 0.06 II: 95.89 \pm 0.14	95.48 \pm 0.04
	I: 55.66 \pm 0.03 II: 96.45 \pm 0.05	I: 55.70 \pm 0.04 II: 96.57 \pm 0.04	I: 55.45 \pm 0.03 II: 96.35 \pm 0.05	I: 55.76 \pm 0.03 II: 96.42 \pm 0.04	I: 54.97 \pm 0.03 II: 96.63 \pm 0.04	96.08 \pm 0.16
4	I: 55.66 \pm 0.03 II: 96.45 \pm 0.05	I: 55.70 \pm 0.04 II: 96.57 \pm 0.04	I: 55.45 \pm 0.03 II: 96.35 \pm 0.05	I: 55.76 \pm 0.03 II: 96.42 \pm 0.04	I: 55.76 \pm 0.03 II: 96.42 \pm 0.04	96.08 \pm 0.16
	I: 55.66 \pm 0.03 II: 96.45 \pm 0.05	I: 55.70 \pm 0.04 II: 96.57 \pm 0.04	I: 55.45 \pm 0.03 II: 96.35 \pm 0.05	I: 55.76 \pm 0.03 II: 96.42 \pm 0.04	I: 55.76 \pm 0.03 II: 96.42 \pm 0.04	96.08 \pm 0.16
5	I: 55.66 \pm 0.03 II: 96.45 \pm 0.05	I: 55.70 \pm 0.04 II: 96.57 \pm 0.04	I: 55.45 \pm 0.03 II: 96.35 \pm 0.05	I: 55.76 \pm 0.03 II: 96.42 \pm 0.04	I: 55.76 \pm 0.03 II: 96.42 \pm 0.04	96.08 \pm 0.16
	I: 55.66 \pm 0.03 II: 96.45 \pm 0.05	I: 55.70 \pm 0.04 II: 96.57 \pm 0.04	I: 55.45 \pm 0.03 II: 96.35 \pm 0.05	I: 55.76 \pm 0.03 II: 96.42 \pm 0.04	I: 55.76 \pm 0.03 II: 96.42 \pm 0.04	96.08 \pm 0.16

Table 1. Results of ADE-Net with Indian Pines (top), KSC (middle), and Houston (bottom) datasets. Best performing results for each attack combination are in bold. Baseline (red) uses a single UNet for training all data combined. X_k values for α_k are dependent on the difficulty of the attack, the specific values can be found in Section 4

Metrics: Two average overall accuracies (OA) terms will be reported: Phase I and Phase II accuracy as shown in Figure 1. The Phase I Discriminator accuracy will be a snapshot of ADE-Net accuracy to determine if attacks are being separated correctly. The Phase II Ensemble accuracy is class-label accuracy and holistically covers ADE-Net classification success.

Evaluation In our experiments, we showcase different hyperparameter values for the discriminator and ensemble terms to find the experimentally optimal values for better ADE-Net accuracy. We also explore the role of CKA by removing it in certain experiments. In the experiment where $\alpha_k = X_k$, values are weighted by the relative difficulty for classification on that attack as: $\alpha_{FGSM} = 1.4$, $\alpha_{CW} = 2.3$, $\alpha_{PGD} = 1.7$, $\alpha_{I-FGSM} = 1.3$, and for vanilla $\alpha_{Vanilla} = 1.0$. Results are found in Table 1 for IP, Kennedy Space Center, and Houston datasets. For all datasets and the number of attacks, ADE-Net outperforms the baseline. As expected, the discriminator performs worse when more attacks are added, however, with the addition of vanilla data in our five attack experiments, we can see the discriminator performing better due to the larger difference between attack data vs vanilla data. For the IP and KSC datasets in general, the highest Phase II accuracy is achieved in our attack dependent α_k tests, showing that giving

more attention to more difficult attacks increases the overall accuracy of ADE-Net. Within ADE-Net for IP and KSC, the No CKA ($\lambda_k = 0$) tests perform worse than all the others, showing the positive effect CKA has on ADE-Net. For the Houston dataset, however, No CKA performs worse only for four attacks and actually performs the best for five attacks. In addition, the attack dependent α_k test only performs the best for four attacks. This could be due to the higher semantic segmentation accuracy for the Houston dataset overall. The added complexity of hyperparameter changes and CKA have little chance to increase accuracy when it is already at roughly 95% for each attack combination. However, ADE-Net still outperforms the single network baseline overall.

5. CONCLUSION

In this paper, we analyze the effect multiple adversarial attacks have on HSI semantic segmentation. An approach was developed leveraging attack-type detection and robustness in one unified network: ADE-Net. Though a Phase I discriminator attack-type classifier leveraging the similarity measure CKA, and a Phase II individual attack expert ensemble network, ADE-Net outperformed the single model baseline for all datasets with all attack combinations.

6. ACKNOWLEDGEMENTS

This work has been partially supported NSF 1920908 (EP-SCoR RII Track-2) and CAREER-NSF 5409260; the findings are those of the authors only and do not represent any position of these funding bodies.

7. REFERENCES

- [1] Battista Biggio, Igino Corona, Davide Maiorca, Blaine Nelson, Nedim Šrndić, Pavel Laskov, Giorgio Giacinto, and Fabio Roli, “Evasion attacks against machine learning at test time,” in *Joint European conference on machine learning and knowledge discovery in databases*. Springer, 2013, pp. 387–402.
- [2] Christian Szegedy, Wojciech Zaremba, Ilya Sutskever, Joan Bruna, Dumitru Erhan, Ian Goodfellow, and Rob Fergus, “Intriguing properties of neural networks,” *arXiv preprint arXiv:1312.6199*, 2013.
- [3] Ian J Goodfellow, Jonathon Shlens, and Christian Szegedy, “Explaining and harnessing adversarial examples,” *arXiv preprint arXiv:1412.6572*, 2014.
- [4] Christian Szegedy, Wojciech Zaremba, Ilya Sutskever, Joan Bruna, Dumitru Erhan, Ian Goodfellow, and Rob Fergus, “Intriguing properties of neural networks,” *arXiv preprint arXiv:1312.6199*, 2013.
- [5] Jan Hendrik Metzen, Tim Genewein, Volker Fischer, and Bastian Bischoff, “On detecting adversarial perturbations,” *arXiv preprint arXiv:1702.04267*, 2017.
- [6] Christian Szegedy, Wojciech Zaremba, Ilya Sutskever, Joan Bruna, Dumitru Erhan, Ian Goodfellow, and Rob Fergus, “Intriguing properties of neural networks,” *arXiv preprint arXiv:1312.6199*, 2013.
- [7] Yonghao Xu, Bo Du, and Liangpei Zhang, “Self-attention context network: Addressing the threat of adversarial attacks for hyperspectral image classification,” *IEEE Transactions on Image Processing*, vol. 30, pp. 8671–8685, 2021.
- [8] Ian J Goodfellow, Jonathon Shlens, and Christian Szegedy, “Explaining and harnessing adversarial examples,” *arXiv preprint arXiv:1412.6572*, 2014.
- [9] Nicholas Carlini and David Wagner, “Towards evaluating the robustness of neural networks,” in *2017 ieee symposium on security and privacy (sp)*. Ieee, 2017, pp. 39–57.
- [10] Aleksander Madry, Aleksandar Makelov, Ludwig Schmidt, Dimitris Tsipras, and Adrian Vladu, “Towards deep learning models resistant to adversarial attacks,” *arXiv preprint arXiv:1706.06083*, 2017.
- [11] Yonghao Xu, Bo Du, and Liangpei Zhang, “Self-attention context network: Addressing the threat of adversarial attacks for hyperspectral image classification,” *IEEE Transactions on Image Processing*, vol. 30, pp. 8671–8685, 2021.
- [12] Sungjune Park, Hong Joo Lee, and Yong Man Ro, “Adversarially robust hyperspectral image classification via random spectral sampling and spectral shape encoding,” *IEEE Access*, vol. 9, pp. 66791–66804, 2021.
- [13] Jiahao Qi, Zhiqiang Gong, Xingyue Liu, Kangcheng Bin, Chen Chen, Yongqian Li, Wei Xue, Yu Zhang, and Ping Zhong, “Masked spatial-spectral autoencoders are excellent hyperspectral defenders,” *arXiv preprint arXiv:2207.07803*, 2022.
- [14] Francesco Croce and Matthias Hein, “Reliable evaluation of adversarial robustness with an ensemble of diverse parameter-free attacks,” in *International conference on machine learning*. PMLR, 2020, pp. 2206–2216.
- [15] Pratyush Maini, Eric Wong, and Zico Kolter, “Adversarial robustness against the union of multiple perturbation models,” in *International Conference on Machine Learning*. PMLR, 2020, pp. 6640–6650.
- [16] Qinzhe Lv, Wei Feng, Yinghui Quan, Gabriel Dauphin, Lianru Gao, and Mengdao Xing, “Enhanced-random-feature-subspace-based ensemble cnn for the imbalanced hyperspectral image classification,” *IEEE Journal of Selected Topics in Applied Earth Observations and Remote Sensing*, vol. 14, pp. 3988–3999, 2021.
- [17] Xin He and Yushi Chen, “Transferring cnn ensemble for hyperspectral image classification,” *IEEE Geoscience and Remote Sensing Letters*, vol. 18, no. 5, pp. 876–880, 2020.
- [18] Praveen Iyer, Sriram A, and Shyam Lal, “Deep learning ensemble method for classification of satellite hyperspectral images,” *Remote Sensing Applications: Society and Environment*, vol. 23, pp. 100580, 2021.
- [19] Rui Bao, Junshi Xia, Mauro Dalla Mura, Peijun Du, Jocelyn Chanussot, and Jinchang Ren, “Combining morphological attribute profiles via an ensemble method for hyperspectral image classification,” *IEEE Geoscience and Remote Sensing Letters*, vol. 13, no. 3, pp. 359–363, 2016.
- [20] Simon Kornblith, Mohammad Norouzi, Honglak Lee, and Geoffrey Hinton, “Similarity of neural network representations revisited,” in *International Conference on Machine Learning*. PMLR, 2019, pp. 3519–3529.
- [21] José Manuel Amigo, “Hyperspectral and multispectral imaging: Setting the scene,” in *Data Handling in Science and Technology*, vol. 32, pp. 3–16. Elsevier, 2020.
- [22] Demetrio Labate, Mohamadkazem Safaripoorfatide, Nikolaos Karantzas, Saurabh Prasad, and Farideh Foroozandeh Shahraki, “Structured receptive field networks and applications to hyperspectral image classification,” 09 2019, p. 23.
- [23] Olaf Ronneberger, Philipp Fischer, and Thomas Brox, “U-net: Convolutional networks for biomedical image segmentation,” in *International Conference on Med-*

ical image computing and computer-assisted intervention. Springer, 2015, pp. 234–241.

[24] Cihang Xie, Zhishuai Zhang, Yuyin Zhou, Song Bai, Jianyu Wang, Zhou Ren, and Alan L Yuille, “Improving transferability of adversarial examples with input diversity,” in *Proceedings of the IEEE/CVF Conference on Computer Vision and Pattern Recognition*, 2019, pp. 2730–2739.